Scientia Iranica B (2021) 28(2), 847–859

SCIENTIA IRANICA

Sharif University of Technology
Scientia Iranica
Transactions B: Mechanical Engineering
http://scientiairanica.sharif.edu

Research Note

A simplified analytical model for predicting the heating performance of single U-tube underground heat exchangers

M. Mohammadian Korouyeh[a], M.H. Saidi[b,*], M. Najafi[a], and C. Aghanajafi[c]

a. *Department of Mechanical Engineering, Tehran Science and Research Branch, Islamic Azad University, Tehran, Iran.*
b. *Center of Excellence in Energy Conversion (CEEC), School of Mechanical Engineering, Sharif University of Technology, Tehran, P.O. Box 11155-9567, Iran.*
c. *School of Mechanical Engineering, K. N. Toosi University of Technology, Tehran, Iran.*

Received 10 February 2019; received in revised form 28 September 2019; accepted 18 January 2020

KEYWORDS
Borehole;
Green's function;
Underground heat exchanger;
Heat transfer rate;
Entropy generation number.

Abstract. To ensure an optimized borehole in terms of heat capacity and cost-effectiveness, it is necessary to predict the heating performance of underground U-tube heat exchangers (boreholes) so that proper parameters such as length, diameter, material, etc. can be designed and selected. To this end, employing reliable equations is essential to predicting the heating performance of a borehole and also, to resolving the design issues. In this study, a single vertical U-tube borehole with a constant wall temperature is considered and analytical equations for temperature distribution in the surrounding ground around the borehole are evaluated based on one- and two-dimensional heat conduction, respectively. The analytical equation is compared with experimental data for a borehole with 50 m depth in which warm water at 40°C is pumped into it within a time period of 120 hours and the heat transfer rate per unit length is recorded. The comparison between analytical expression and experimental data shows good agreement between them. Also, the borehole entropy generation number is studied and the optimized parameters are evaluated to minimize it. It is concluded that for the considered borehole, the entropy generation number decreases upon an increase in its length and a decrease in the borehole radius and pipe outer radius.

1. Introduction

Geothermal energy is one of the important renewable energies that is clean, sustainable, and generally available in different parts of the world. Due to slight variation in ground temperature than ambient temperature, ground can absorb heat in hot seasons and inject heat to the considered space in the cold seasons. Therefore, boreholes in the form of underground heat exchangers have attracted much attention as a medium to exchange heat between space and the ground. U-tube heat exchangers are dipped in the ground and then, filled with grout. The flowing fluid is a medium that exchanges heat load with the surrounding ground. Evaluation of the borehole heating performance is an integral part of the borehole design that may help predict its ability to handle part of the required energy.

*. *Corresponding author. Tel.: +98 21 66165522*
E-mail addresses: msd.mohammadian@srbiau.ac.ir (M. Mohammadian Korouyeh); saman@sharif.edu (M.H. Saidi); mnajafi38@yahoo.com (M. Najafi); aghanajafi@kntu.ac.ir (C. Aghanajafi)

doi: 10.24200/sci.2020.52905.2945

One of the important issues of the borehole design is economical evaluation given that its lifetime may decrease due to inappropriate size selection. Heat transfer rate evaluation may help estimate borehole specifications. There are several models including analytical or numerical ones that can predict heating performance.

The infinite line source model [1] and the cylindrical source model [2] represent two analytical solutions that may evaluate the long-term thermal performance of the borehole heat exchanger. Heat conduction in the vertical direction is neglected in both models and it is assumed that the wall is imposed with constant heat flux. Eskilson [3] used a two-dimensional finite difference model to consider the effect of the finite borehole length. In his proposed model, wall temperature was presented in terms of non-dimensional thermal response functions, known as g-function. Zeng et al. [4] suggested a two-dimensional analytical solution for the heat conduction in the ground, which is called finite line-source model. Similar to the previous analytical solutions [1,2], the heating load was assumed constant along the borehole. Aydin et al. [5] used a one-dimensional heat transfer model to analyze the borehole. They used Laplace transform to predict temperature distribution outside of the borehole and estimate heat transfer rate per unit length. They validated their calculations based on the results derived from COMSOL software outputs. Also, they stated that analysis of boreholes with a constant wall temperature was more accurate than that with wall under constant heat flux. Biglarian et al. [6] proposed a numerical model to simulate heat transfer in a single borehole heat exchanger. They employed 2D finite volume for the outside of the borehole and resistance capacity model for the inside of the borehole. Lee and Lam [7] developed a 3D fully implicit finite difference model in rectangular coordinates. They calculated the wall temperature and heating load along the borehole. Minaei and Marefat [8] presented an analytical model to predict the short-term heating performance of boreholes. Several researchers have developed an analytical equation based on Green's function in Cartesian coordinates for infinite boundaries [9–11]. They evaluated the rate of heat transfer being carried by the borehole. Lee and Lam [12] used a 2×2 ground heat exchanger and simulated the year-round dynamic performance using TRNSYS. They showed that the application of displacement ventilation offered 23% more energy saving than the mixing ventilation. Saeidi et al. [13] modeled the heat pump with a ground heat source and evaluated its thermodynamic performance. They considered horizontal and vertical ground heat exchangers and concluded that using R512a, R600, and R717 might be the most proper substitute refrigerants in the geothermal heat pumps from both economic and environmental viewpoints. Kummert and Bernier [14] presented a simulation study of closed-loop ground coupled heat pump systems for a typical residential building in North America. They compared the results obtained from TRNSYS with the models that took dynamic into account in the geothermal fluid loop within the borehole. Beier and Holloway [15] determined variations of the ground conductivity and borehole resistance to a set of horizontal boreholes over a two-year period. They found that ground thermal conductivity was increased upon increase in the depth. Mensah et al. [16] proposed a numerical simulation of the optimal design of boreholes based on the building load and validated the simulation analysis with experimental data. Cimmino [17] presented an analytical model by using Laplace transform method to calculate fluid temperature in boreholes. Their proposed model had good agreement with finite difference method. Dehkordi et al. [18] found that tight boreholes might provide an acceptable heating performance while civil works would be decreased. Tang and Nowamooz [19] analyzed the long-term performance of shallow borehole heat exchangers. They found that yearly total extracted energy would be decreased annually. Also, they showed that this reduction became less significant after the fourth year. Monzó et al. [20] employed a numerical model considering the effect of thermal resistance between the fluid and the borehole wall. Zhang et al. [21] presented an optimization design methodology with the Hooke-Jeeves pattern search algorithm in order to size and design underground heat exchangers under a given annual cooling and heating load. They found that when inlet fluid temperature was decreased from 5°C to 0°C, the total borehole length required for installing single underground heat exchangers was reduced by 13.3%. Li et al. [22] developed a numerical model considering five strata and presented the axial temperature profiles of different layers at different distances. They showed that the layered subsurface and groundwater flow played a non-negligible role in evaluating the performance of borehole heat exchangers. Holmberg et al. [23] studied the performance of deep coaxial borehole heat exchangers. They showed that the heat load extracted from boreholes was significantly increased by increasing borehole depth. Moreover, they presented a chart as guide when sizing deep coaxial boreholes. Beier et al. [24] applied a borehole heat transfer model that used a transient weighting factor to calculate an average circulating fluid temperature along the borehole.

The main objective of this study is to evaluate the heating operation of boreholes to predict its ability to carry heating load. In this research, a single U-tube underground heat exchanger is considered. A new analytical solution based on Green's function is proposed to calculate the temperature distribution outside of the

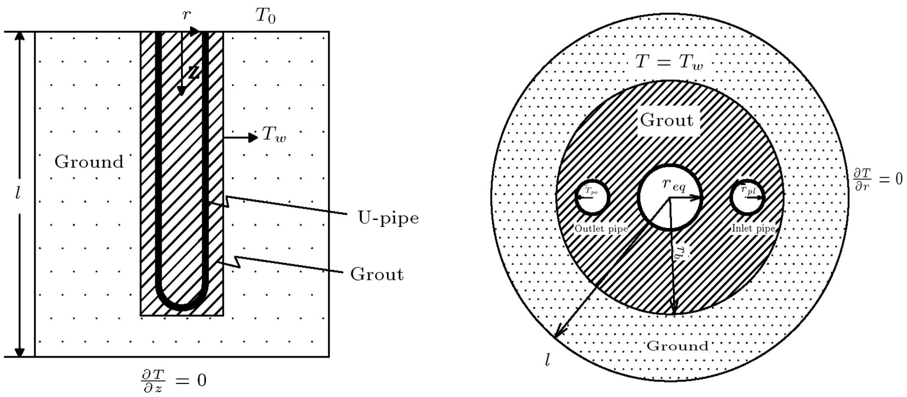

Figure 1. Schematic of the borehole.

borehole and estimate its heating transfer rate capacity. The borehole wall temperature is considered constant. The results are compared to experimental data in which good agreement between them has been concluded.

Moreover, genetic algorithm is applied to optimize borehole in terms of entropy generation minimization. The non-dimensional form of entropy generation (Entropy Generation Number (EGN)) is selected as an objective function and the optimum technical parameters are calculated to have the minimum EGN.

2. Problem description

Here, heat conduction in the ground is evaluated. Since there is no fluid flow, there is no heat convection and only heat conduction between the borehole and the ground occurs. Heat transfer depends on the ground, grout, and the pipe materials and also the type of working fluid. It is assumed that all the materials are homogeneous for heat transfer modeling.

By neglecting temperature variations in the tangential direction, 2D heat conduction in cylindrical coordinates is used as follows:

$$\frac{\partial^2 T}{\partial z^2} + \frac{1}{r}\frac{\partial}{\partial r}\left(r\frac{\partial T}{\partial r}\right) = \frac{1}{\alpha_{\text{ground}}}\frac{\partial T}{\partial t}. \tag{1}$$

To model the borehole, it is assumed that wall temperature is constant due to better accuracy and shorter time to reach the steady state regime [5,9,25,26].

Temperature distribution in the ground will be evaluated by solving the heat conduction equation. In practice, boreholes are characterized by a radius between 0.03 m and 0.5 m and a length between 40 m and 200 m [10]. Since the borehole diameter is of less significance than its length by comparison, the one-dimensional mathematical model can be used in the radial direction [9,25]. Eskilson [3] suggested that the axial heat transfer could be neglected for $t < L^2/90\alpha$.

Therefore, the 2D model is applied to analyze temperature distribution in the surrounding ground around the borehole. In this model, it is assumed that in the horizontal and vertical far fields, equal to infinity, there is no heat gradient in the r and z directions: $\frac{\partial T}{\partial r} = 0$ and $\frac{\partial T}{\partial z} = 0$, respectively.

In this study, the main goal is to calculate the amount of heat being exchanged between borehole and the ground. For this purpose, the system and its related boundary conditions are considered in Figure 1.

As mentioned earlier, 1D and 2D heat conduction is used and Green's function is applied to calculate temperature distribution in the ground and estimate the amount of heat being exchanged between the ground and the borehole.

3. Mathematical model

3.1. Temperature distribution

3.1.1. One-dimensional solution

Considering the previous assumptions, the one-dimensional form of heat conduction (ignoring axial heat conduction) was used. Therefore, the one-dimensional form of Eq. (1) can be written as follows:

$$\frac{\partial^2 T}{\partial r^2} + \frac{1}{r}\frac{\partial T}{\partial r} = \frac{1}{\alpha_{\text{ground}}}\frac{\partial T}{\partial t}, \qquad r_b < r < r_b + l, \quad t > 0. \tag{2}$$

The related boundary and the initial conditions are given by:

$$T(r = r_b, t) = T_w, \tag{3}$$

$$\left.\frac{\partial T}{\partial r}\right]_{r=r_b+l} = 0, \tag{4}$$

$$T(r, t = 0) = T_0, \tag{5}$$

where α_{ground} is the ground thermal diffusivity, T_w is the borehole wall temperature, r_b equals the borehole radius, T_0 is initial temperature, and l is the horizontal far field distance at which the temperature variation in the radial direction (at that point) is insignificant.

Biglarian et al. [6] considered l equal to $5\sqrt{\alpha t_{\max}}$ in which $t_{\max}$ denotes the duration of the simulation process. By replacing $T-T_0$ into $\tilde{T}$, Eqs. (2) to (5) are replaced as follows:

$$\frac{\partial^2 \tilde{T}}{\partial r^2}+\frac{1}{r}\frac{\partial \tilde{T}}{\partial r}=\frac{1}{\alpha_{\text{ground}}}\frac{\partial \tilde{T}}{\partial t}, \tag{6}$$

$$\tilde{T}(r=r_b,t)=T_w-T_0=T_{w1}, \tag{7}$$

$$\frac{\partial \tilde{T}}{\partial r}_{r=r_b+l}=0, \tag{8}$$

$$\tilde{T}(r,t=0)=0. \tag{9}$$

Dimensionless forms of Eqs. (6) to (9) are given by:

$$\frac{\partial^2 \bar{T}}{\partial \bar{r}^2}+\frac{1}{\bar{r}}\frac{\partial \bar{T}}{\partial \bar{r}}=\frac{\partial \bar{T}}{\partial \bar{t}}, \qquad 1<\bar{r}<\bar{R}, \qquad \bar{t}>0, \tag{10}$$

$$\bar{T}\left(1,\bar{t}\right)=1, \tag{11}$$

$$\frac{\partial \bar{T}}{\partial \bar{r}}\left(\bar{R},\bar{t}\right)=0, \tag{12}$$

$$\bar{T}\left(\bar{r},0\right)=0. \tag{13}$$

The dimensionless parameters are defined as follows:

$$\bar{T}=\frac{\tilde{T}}{T_{w1}}, \tag{14}$$

$$\bar{r}=\frac{r}{r_b}, \tag{15}$$

$$\bar{R}=\frac{r_b+l}{r_b}, \tag{16}$$

$$\bar{t}=\frac{\alpha_{\text{ground}}t}{r_b^2}. \tag{17}$$

The expression of Green's function for the hollow cylinder in which the inner temperature equals a constant temperature and the outer surface is insulated can be found as follows [27]:

$$G\left(r,t,r',\tau\right)=\frac{\pi}{4}\sum_{m=1}^{\infty}e^{-\beta_m^2(t-\tau)}\frac{\beta_m^2 J_0^2(\beta_m)}{J_0^2(\beta_m)-J_1^2\left(\beta_m\bar{R}\right)}$$
$$\times\left[J_0(\beta_m r)Y_1\left(\beta_m\bar{R}\right)-J_1\left(\beta_m\bar{R}\right)Y_0(\beta_m r)\right]$$
$$\times\left[J_0\left(\beta_m r'\right)Y_1\left(\beta_m\bar{R}\right)-J_1\left(\beta_m\bar{R}\right)Y_0\left(\beta_m r'\right)\right]. \tag{18}$$

This function is applied to solve Eq. (10) to find the analytical expression for temperature distribution.

In the above equation, J_0 is the first-kind Bessel's function of zeroth order, J_1 is the first-kind Bessel's function of 1st order, Y_0 is the second-kind Bessel's function of zeroth order, Y_1 is the second-kind Bessel's function of 1st order, and β_m is the eigenvalue. Temperature distribution can be found using Green's function rules as follows:

$$T(r,t)=\int_{\tau=0}^{t}\left.\frac{\partial G}{\partial r'}\right]_{r'=1}2\pi r_i d\tau. \tag{19}$$

Therefore, dimensionless temperature distribution is given by the following expression:

$$\bar{T}=-\frac{\pi^2}{2}\sum_{m=1}^{\infty}\left[1-e^{-\beta_m^2\bar{t}}\right]\frac{\beta_m J_0^2(\beta_m)}{J_0^2(\beta_m)-J_1^2\left(\beta_m\bar{R}\right)}$$
$$\left(J_0\left(\beta_m\bar{r}\right)Y_1\left(\beta_m\bar{R}\right)-J_1\left(\beta_m\bar{R}\right)Y_0\left(\beta_m\bar{r}\right)\right)$$
$$\times\left(J_1(\beta_m)Y_1\left(\beta_m\bar{R}\right)-J_1\left(\beta_m\bar{R}\right)Y_1\left(\beta_m\right)\right). \tag{20}$$

On the one hand, the steady state solution to Eq. (10) is given below:

$$T_s=1. \tag{21}$$

On the other hand, the steady state of Eq. (20) can be calculated in the limit as $\bar{t}\to\infty$ in the following:

$$T_s=-\frac{\pi^2}{2}\sum_{m=1}^{\infty}\frac{\beta_m J_0^2(\beta_m)}{J_0^2(\beta_m)-J_1^2\left(\beta_m\bar{R}\right)}$$
$$\left(J_0\left(\beta_m\bar{r}\right)Y_1\left(\beta_m\bar{R}\right)-J_1\left(\beta_m\bar{R}\right)Y_0\left(\beta_m\bar{r}\right)\right)$$
$$\times\left(J_1(\beta_m)Y_1\left(\beta_m\bar{R}\right)-J_1\left(\beta_m\bar{R}\right)Y_1(\beta_m)\right). \tag{22}$$

Therefore, dimensionless temperature distribution is given by the following expression:

$$\bar{T}=1+\frac{\pi^2}{2}\sum_{m=1}^{\infty}e^{-\beta_m^2\bar{t}}\frac{\beta_m J_0^2(\beta_m)}{J_0^2(\beta_m)-J_1^2\left(\beta_m\bar{R}\right)}$$
$$\left(J_0\left(\beta_m\bar{r}\right)Y_1\left(\beta_m\bar{R}\right)-J_1\left(\beta_m\bar{R}\right)Y_0\left(\beta_m\bar{r}\right)\right)$$
$$\times\left(J_1(\beta_m)Y_1\left(\beta_m\bar{R}\right)-J_1\left(\beta_m\bar{R}\right)Y_1(\beta_m)\right). \tag{23}$$

β_m (eigenvalue) can be evaluated by applying the boundary condition of Eq. (11) in Eq. (23). The result may be found by solving the following equation:

$$J_0(\beta_m)Y_1\left(\beta_m\bar{R}\right)-J_1\left(\beta_m\bar{R}\right)Y_0\left(\beta_m\right)=0. \tag{24}$$

Eq. (24) may be solved by applying Householder's iteration method, which is calculated using a modified homotopy perturbation method for nonlinear equations as in the following equation [28]:

$$x_{n+1}=x_n-\frac{f(x_n)}{f'(x_n)}-\frac{f^2(x_n)f''(x_n)}{2f'^3(x_n)}. \tag{25}$$

Figure 2 shows temperature variations in the surrounding ground around the borehole upon an increase in

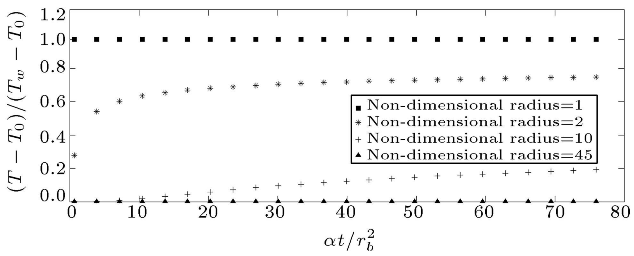

Figure 2. Temperature distribution vs. time in the surrounding ground.

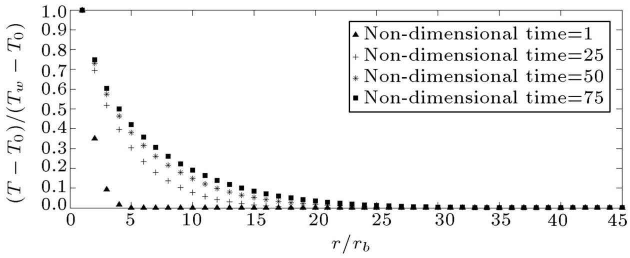

Figure 3. Temperature distribution vs. distance from the borehole on different time scales.

the time duration in several radiuses. It is shown that ground temperature of each location increases with increasing the time duration due to heat penetration. As mentioned earlier, temperature variation in far field ($\bar{r}=45$) is insignificant and the temperature equals T_0.

Figure 3 shows temperature variations around the borehole with increasing the non-dimensional radius in several time steps. It is shown that ground temperature decreases with increase in the distance from the borehole in each time step due to the reduced borehole effects at far-field points and also, the far-field temperature approximately equals T_0. Moreover, as time passes, borehole effects disappear at far enough distances from the borehole and the temperature in those places reaches T_0.

3.1.2. Two-dimensional solution

In this part, the horizontal and vertical far fields are assumed equal to infinity and at those points, there is no temperature gradient (Eqs. (42) and (43)). Furthermore, the axial heat conduction (in the z direction) is considered and as a result, Eq. (1) may be applied. To evaluate the temperature distribution, Green's function in an infinite medium is applied [9–11,29], which is defined as the function of temperature raise caused by a heat source that is located at point (x', y', z') and activated at instant t'. This function in the Cartesian coordinates is shown in the given equation:

$$G\left(x,y,z,t;x',y',z',t'\right)=\frac{1}{8\left(\pi\alpha\left(t-t'\right)\right)^{\frac{3}{2}}}\exp\left(-\frac{\left(x-x'\right)^2+\left(y-y'\right)^2+\left(z-z'\right)^2}{4\alpha\left(t-t'\right)}\right). \quad (26)$$

A point (x,y,z) in the Cartesian coordinates may be changed to (r,φ,z) in the cylindrical coordinates. The conversion would be done by applying $x=r\cos\varphi$, $y=r\sin\varphi$ and $z=z$. Therefore, Green's function in the cylindrical coordinates is given by Eq. (27) as shown in Box I. By using Green's function rules, the temperature rise distribution in the ground as the infinite medium may be as follows [9]:

$$T(r,\varphi,z,t)-T_0=\int_0^{2\pi}d\varphi'\int_{-\infty}^{+\infty}dz'\int_0^t BG\left(r,\varphi,z,t:r',\varphi',z',t'\right)dt'. \quad (28)$$

B is a variable which is a function of boundary conditions [9]. Various problems may have different B quantities. In the current problem, the borehole wall temperature is assumed constant.

Since 2D heat conduction is studied and the temperature distribution is independent of angular coordinate, $\varphi=0$ and this temperature rise can be calculated as follows:

$$T(r,z,t)-T_0=\int_0^{2\pi}d\varphi'\int_{-\infty}^{+\infty}dz'\int_0^t\frac{B}{8\left(\pi\alpha\left(t-t'\right)\right)^{\frac{3}{2}}}\exp\left(-\frac{r^2+r_b^2-2rr_b\cos\varphi'+\left(z-z'\right)^2}{4\alpha\left(t-t'\right)}\right)dt'. \quad (29)$$

Integral of the angular part is calculated as follows:

$$\int_0^{2\pi}\exp\left(\frac{2rr_b\cos\varphi'}{4\alpha\left(t-t'\right)}\right)d\varphi'=2\pi I_0\left(\frac{rr_b}{2\alpha\left(t-t'\right)}\right). \quad (30)$$

To analyze the borehole, it is assumed that ground surface keeps a constant temperature as its initial

$$G\left(r,\varphi,z,t:r',\varphi',z',t'\right)=\frac{1}{8\left(\pi\alpha\left(t-t'\right)\right)^{\frac{3}{2}}}\exp\left(-\frac{\left(r\cos\varphi-r'\cos\varphi'\right)^2+\left(r\sin\varphi-r'\sin\varphi'\right)^2+\left(z-z'\right)^2}{4\alpha\left(t-t'\right)}\right). \quad (27)$$

Box I

temperature (T_0). Therefore, a virtual heating sink is assumed on symmetry to the boundary.

The solution to Eq. (29) may be written as in the following equation:

$$T - T_0 = \int_0^t \frac{B}{8\left(\pi\alpha\left(t-t'\right)\right)^{\frac{3}{2}}} 2\pi I_0\left(\frac{r r_b}{2\alpha\left(t-t'\right)}\right) \exp\left(-\frac{r^2+r_b^2}{4\alpha\left(t-t'\right)}\right)\left\{\int_0^h \exp\left(-\frac{\left(z-z'\right)^2}{4\alpha\left(t-t'\right)}\right) dz' - \int_{-h}^0 \exp\left(-\frac{\left(z-z'\right)^2}{4\alpha\left(t-t'\right)}\right) dz'\right\} dt'. \tag{31}$$

To solve the above equation, the following relations are applied:

$$\int \exp\left(-\frac{z^2}{b^2}\right) dz = \frac{\sqrt{\pi}}{2} b\, erf\left(\frac{z}{b}\right) + \text{constant}, \tag{32}$$

$$erf(z) = \frac{2}{\sqrt{\pi}} \int_0^z \exp\left(-t^2\right) dt, \tag{33}$$

$$erf(-z) = -erf(z). \tag{34}$$

Therefore, the solution to Eq. (31) can be written by:

$$T(r,z,t) - T_0 = \int_0^t \frac{B}{4\alpha\left(t-t'\right)} I_0\left(\frac{r r_b}{2\alpha\left(t-t'\right)}\right) \exp\left(-\frac{r^2+r_b^2}{4\alpha\left(t-t'\right)}\right)\left\{erf\left(\frac{h-z}{2\sqrt{\alpha\left(t-t'\right)}}\right) + 2erf\left(\frac{z}{2\sqrt{\alpha\left(t-t'\right)}}\right) - erf\left(\frac{h+z}{2\sqrt{\alpha\left(t-t'\right)}}\right)\right\} dt'. \tag{35}$$

Eq. (35) is the modified form of the mathematical equation, which was proposed by Dehghan [11]. The 2D solution of temperature distribution in the ground may be shown in the non-dimensional form by defining the following parameters:

$$\bar{h} = \frac{h}{r_b}, \tag{36}$$

$$\bar{z} = \frac{z}{h}, \tag{37}$$

$$\bar{t}' = \frac{\alpha t'}{r_b^2}. \tag{38}$$

By applying the above relations and Eqs. (14), (15), and (17), the related non-dimensional initial and boundary conditions are given by:

$$\bar{T}\left(\bar{r},\bar{z},0\right) = 0, \tag{39}$$

$$\bar{T}\left(1,\bar{z},\bar{t}\right) = 1, \tag{40}$$

$$\bar{T}\left(\bar{r},0,\bar{t}\right) = 0, \tag{41}$$

$$\left.\frac{\partial \bar{T}\left(\bar{r},\bar{z},\bar{t}\right)}{\partial \bar{r}}\right|_{\bar{r}\to\infty} = 0, \tag{42}$$

$$\left.\frac{\partial \bar{T}\left(\bar{r},\bar{z},\bar{t}\right)}{\partial \bar{z}}\right|_{\bar{z}\to\infty} = 0. \tag{43}$$

Therefore, by considering Eqs. (39)–(43), the non-dimensional form of Eq. (35) will be Eq. (44) which is shown in Box II. The mathematical relation in Eq. (44) is another form of the temperature distribution equation, which was reported by Dehghan [11], due to the non-dimensional parameter definition.

To analyze Eq. (44), a MATLAB code is developed and the results can be seen in Figures 4–6.

Figure 4 shows temperature variations upon increase in the time duration in several radiuses. It is shown that the ground temperature in each location increases upon increase in the time duration due to heat penetration, which is compatible with data in Figure 2.

Figure 5 shows temperature distribution variations around the borehole with increasing the distance in several time steps. Similar to the 1D analysis, it is shown that ground temperature would be decreased by increasing distance from the borehole in each time step because borehole effects are reduced at the far-field points. Moreover, the results shown in Figure 5 are compatible with the data in Figure 3.

$$\bar{T} = \frac{T(r,z,t) - T_0}{T_w - T_0} = \frac{\int_0^{\bar{t}} \frac{1}{(\bar{t}-\bar{t}')} I_0\left(\frac{\bar{r}}{2(\bar{t}-\bar{t}')}\right) \exp\left(-\frac{1+\bar{r}^2}{4(\bar{t}-\bar{t}')}\right)\left\{erf\left(\frac{\bar{h}(1-\bar{z})}{2\sqrt{(\bar{t}-\bar{t}')}}\right) + 2erf\left(\frac{\bar{h}\bar{z}}{2\sqrt{(\bar{t}-\bar{t}')}}\right) - erf\left(\frac{\bar{h}(1+\bar{z})}{2\sqrt{(\bar{t}-\bar{t}')}}\right)\right\} d\bar{t}'}{\int_0^{\bar{t}} \frac{1}{(\bar{t}-\bar{t}')} I_0\left(\frac{1}{2(\bar{t}-\bar{t}')}\right) \exp\left(-\frac{1}{2(\bar{t}-\bar{t}')}\right)\left\{erf\left(\frac{\bar{h}(1-\bar{z})}{2\sqrt{(\bar{t}-\bar{t}')}}\right) + 2erf\left(\frac{\bar{h}\bar{z}}{2\sqrt{(\bar{t}-\bar{t}')}}\right) - erf\left(\frac{\bar{h}(1+\bar{z})}{2\sqrt{(\bar{t}-\bar{t}')}}\right)\right\} d\bar{t}'}. \tag{44}$$

Box II

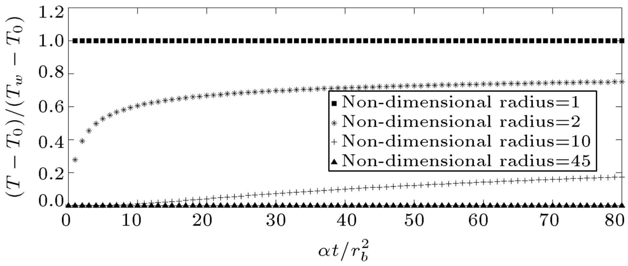

Figure 4. Temperature distribution vs. time in the surrounding ground.

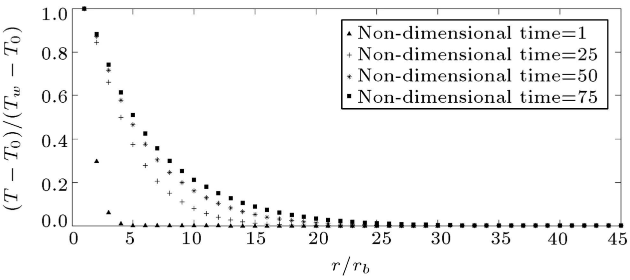

Figure 5. Temperature distribution vs. distance from the borehole on different time scales.

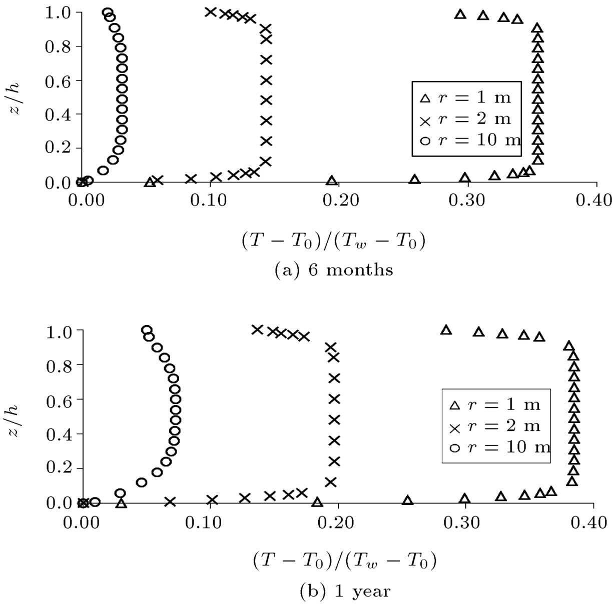

Figure 6. Temperature distribution vs. ground depth at various distances after (a) 6 months and (b) 1 year.

Figure 6(a) and (b) show the temperature distribution variations with increasing the borehole depth after 6 months and 1 year, respectively.

As shown earlier, on the ground surface, we have $T = T_0$ and by dipping into ground, the temperature increases first and then, decreases. Also, it is shown that for each time step and each depth, ground temperature increases with decrease in the distance to the borehole. For each location, the temperature increases over the course of 6 months to 1 year due to heat penetration.

3.2. Heat transfer rate per unit length

One of the important parts of this study is calculating the heating transfer rate per unit length between the ground and the borehole. For this purpose, 1D dimensionless heat transfer rate per unit length outside of the borehole can be calculated as follows:

$$\bar{q} = \frac{q_b}{2\pi k_{\text{ground}} T_{w1}} = -\frac{\partial \bar{T}}{\partial \bar{r}}\bigg]_{\bar{r}=1}, \tag{45}$$

$$\bar{q} = -\frac{\pi^2}{2}\sum_{m=1}^{\infty} e^{-\beta_m^2 \bar{t}} \frac{\beta_m^2 J_0^2(\beta_m)}{J_0^2(\beta_m) - J_1^2\left(\beta_m \bar{R}\right)}$$

$$\left(J_1\left(\beta_m \bar{R}\right) Y_1\left(\beta_m\right) - J_1(\beta_m) Y_1\left(\beta_m \bar{R}\right)\right)$$

$$\times \left(J_1(\beta_m) Y_1\left(\beta_m \bar{R}\right) - J_1\left(\beta_m \bar{R}\right) Y_1(\beta_m)\right). \tag{46}$$

Therefore, 2D dimensionless heat transfer rate per unit length outside of the borehole can be calculated as follows:

$$\bar{q} = -\frac{\partial \bar{T}}{\partial \bar{r}}\bigg|_{\bar{r}=1}$$

$$= \frac{\int_0^{\bar{t}} \frac{1}{(\bar{t}-\bar{t}')} A_1 A_2 d\bar{t}'}{\int_0^{\bar{t}} \frac{1}{(\bar{t}-\bar{t}')} A_2 I_0\left(\frac{1}{2(\bar{t}-\bar{t}')}\right) \exp\left(-\frac{1}{2(\bar{t}-\bar{t}')}\right) d\bar{t}'}. \tag{47}$$

Coefficients A_1 and A_2 may be shown in Eqs. (48) and (49).

$$A_1 = \frac{1}{2(\bar{t}-\bar{t}')} \exp\left(-\frac{1}{2(\bar{t}-\bar{t}')}\right) \left(I_1\left(\frac{1}{2(\bar{t}-\bar{t}')}\right)\right.$$

$$\left.\left. -I_0\left(\frac{1}{2(\bar{t}-\bar{t}')}\right)\right)\right), \tag{48}$$

$$A_2 = erf\left(\frac{\bar{h}(1-\bar{z})}{2\sqrt{(\bar{t}-\bar{t}')}}\right) + 2erf\left(\frac{\bar{h}\bar{z}}{2\sqrt{(\bar{t}-\bar{t}')}}\right)$$

$$- erf\left(\frac{\bar{h}(1+\bar{z})}{2\sqrt{(\bar{t}-\bar{t}')}}\right). \tag{49}$$

In addition, the heat transfer rate per unit length between inside of the borehole and its wall is given by:

$$q_b = \frac{T_{avr.} - T_w}{\frac{\ln\frac{r_b}{r_{eq}}}{2\pi k_{grout}} + \frac{\ln\frac{r_{po}}{r_{pi}}}{4\pi k_{pipe}} + \frac{1}{h_i \times 4\pi r_{pi}}}, \tag{50}$$

where $T_{avr.}$ equals he fluid mean temperature $T_{avr.} = (T_{in} + T_{out})/2$, T_w is the borehole wall temperature,

$r_{eq.}$ equals the equivalent radius ($r_{eq.} = \sqrt{2}r_{po}$) [30], r_{po} is the outer pipe radius, r_{pi} is the inner pipe radius, r_b is the borehole radius, k_{grout} is the grout thermal conductivity coefficient, k_{pipe} is the pipe thermal conductivity coefficient, and h_i is the convective heat transfer coefficient. It is worth mentioning that the equivalent pipe is characterized by an outer surface equal to the sum of outer surfaces of both pipes and thermal resistance of the equivalent pipe (from the fluid to outer surface) equal to that of two pipes in the parallel form.

In addition, the rate of heat transfer per unit length that fluid transfers to the borehole and the ground can be calculated using the following expression:

$$q_f = \frac{\dot{m}c_{p,\text{water}}}{h}\left(T_{in} - T_{out}\right), \tag{51}$$

where $\dot{m}$ is the fluid mass flow rate, $c_{p,\text{water}}$ is the fluid heat capacity, h is the borehole length, T_{in} is the inlet fluid temperature that is pumped into the borehole, and T_{out} is the outlet fluid temperature that exits the borehole.

In order to calculate the convective heat transfer coefficient, h_i, it may be calculated using the following expression:

$$h_i = \frac{\text{Nu} \times k_f}{d_{pi}}. \tag{52}$$

Nu is the Nusselt number calculated through the following equation [31]:

$$\text{Nu} = 0.023\text{Re}^{0.8}\text{Pr}^{0.3}, \tag{53}$$

where:

$$\text{Re} = \frac{2\dot{m}}{\pi r_{pi}\mu_f}. \tag{54}$$

Eq. (53) holds for Re > 2300. For Re < 2300 and for internal flows facing constant temperature, Nu number is constant and Nu = 3.66.

As it is seen, grout, pipe, and ground specifications as well as the working fluid type are included in q calculation.

4. Results

4.1. Validation of analytical solution

In order to validate the analytical results, experimental data of a single U-tube borehole [9] are applied. Test specification is shown in Table 1. To record the test result, water is heated to 40°C through electrical resistance and related valves are opened and water flows into the borehole at a constant temperature. Then, heat transfer rate per unit length is calculated using Eq. (51).

Table 1. Test conditions of the single U-tube borehole.

Parameters	Value
Thermal properties of ground	
ρ_{ground}	2100 kg/m^3
$c_{p,\text{ground}}$	800 J/kg K
k_{ground}	3 W/m K
Thermal properties of grout	
ρ_{grout}	1352 kg/m^3
$c_{p,\text{grout}}$	900 J/kg K
k_{grout}	2.1 W/m K
Thermal properties of water	
ρ_{water}	998 kg/m^3
$c_{p,\text{water}}$	4179 J/kg K
k_{water}	0.627 W/m K
μ_{water}	0.00067 kg/(m.s)
Pipe properties	
ρ_{pipe}	950 kg/m^3
$c_{p,\text{pipe}}$	2300 J/kg K
k_{pipe}	0.4 W/m K
r_{po}	0.016 m
r_{pi}	0.013 m
Working conditions	
h	50 m
r_b	0.1 m
Fluid flow mass flow rate	0.355 kg/s
T_0	16 C
T_{in}	40 C
Simulation time	120 hours

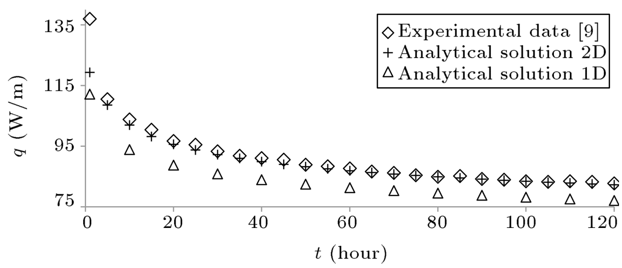

Figure 7. Heat transfer rate per unit length vs. time.

Figure 7 shows the analytical solution of heat transfer rate per unit length. As it is seen, analytical solutions have a good trend with experimental data.

Moreover, the borehole heat transfer rate per unit length decreases upon an increase in temperature around the borehole.

4.2. Long-term performance prediction

Heat transfer rate per unit length is calculated analytically and is compared with experimental data for

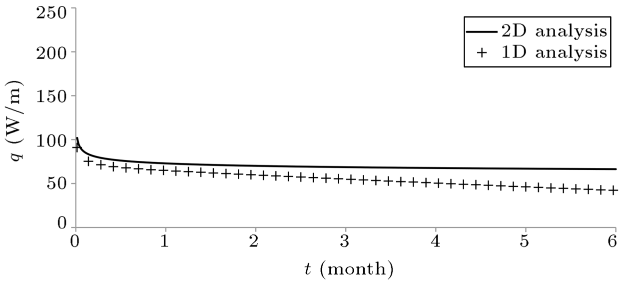

Figure 8. Heat transfer rate per unit length vs. time for long-term performance prediction.

120 hours. The difference between analytical and experimental data is in a good range. It is beneficial to predict the long-time continuous operation of the borehole. Figure 8 shows the 6-month nonstop operation of the borehole. In real cases, borehole works in the on/off mode and does not work continuously. Therefore, this result is the worst case scenario and it can be used to predict borehole performance to select appropriate borehole specifications.

As it is seen, in long terms, 1D and 2D solutions are in good agreement and they are separated due to axial heat conduction over the longer period of time.

4.3. Flow regime effect

Flow regime is a factor that can affect heat transfer. In the turbulent flow, h_i is calculated using Eq. (53) and in the laminar flow, h_i is calculated from Nu = 3.66. Figure 9 shows heat transfer rate per unit length for several mass flow rates and Re numbers.

It is shown that for lower Re numbers, q is approximately constant in each time step and q changes with time at higher Re numbers. In addition, for $\dot{m}_f > 0.355$ kg/s, heat transfer rate per unit length varies fairly by increasing both $\dot{m}_f$ and Re number.

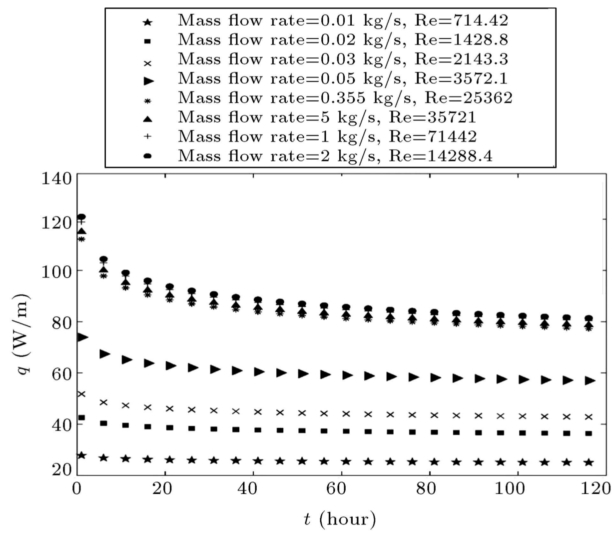

Figure 9. Heat transfer rate per unit length vs. time for different mass flow rates.

4.4. Borehole length effect

Figures 10 and 11 show the effect of length on borehole performance. According to Figure 10, heat transfer rate per unit length has decreased upon increase in borehole length. According to Figure 11, heat transfer rate (Q) increases when the borehole length increases.

4.5. Entropy generation

The irreversibility source of a borehole consists of heat transfer and pressure drop. It is highly desirable to optimize the borehole; therefore, entropy generation minimization becomes the objective function.

Entropy generation due to temperature difference may be written as follows [32]:

$$S_{gen,\Delta T} = \frac{Q\Delta T}{T_{f,m}^2(1+\chi)}. \tag{55}$$

Q is the heat transfer rate and it is calculated using the 1D solution. ΔT is temperature difference between logarithmic average fluid flow temperature and the wall temperature ($T_{f,m} - T_w$). $T_{f,m}$ and χ may be calculated using Eqs. (56) and (57).

$$T_{f,m} = \frac{T_{in} - T_{out}}{\ln \frac{T_{in}}{T_{out}}}, \tag{56}$$

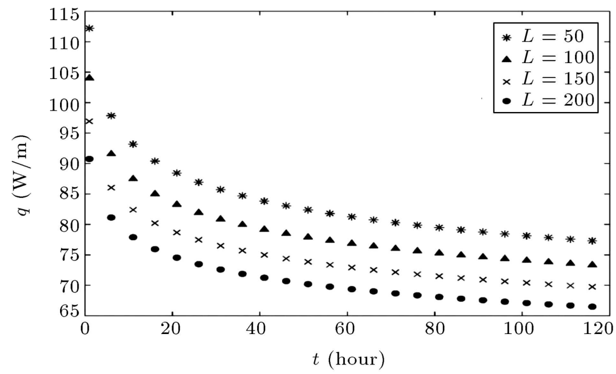

Figure 10. Heat transfer rate per unit length vs. time for different borehole lengths.

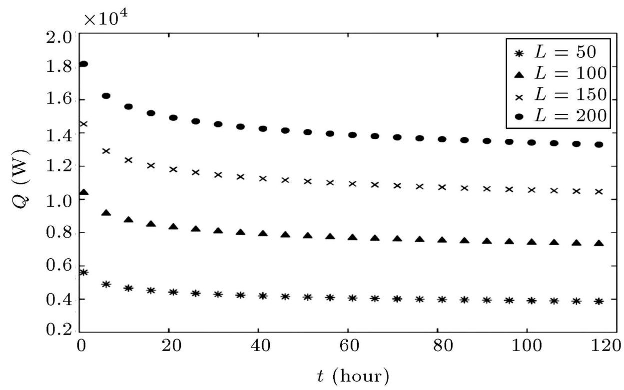

Figure 11. Heat transfer rate vs. time for different borehole lengths.

$$\chi = \frac{\Delta T}{T_{f,m}}. \tag{57}$$

Entropy generation due to the pressure drop is calculated through the following equation [32]:

$$S_{gen,\Delta p} = \frac{\dot{m}_f \Delta p}{\rho_f T_{f,m}}. \tag{58}$$

Δp is the pressure drop in the pipe that is given by:

$$\Delta p = \frac{f \dot{m}_f^2 (2h)}{\rho_f \pi^2 r_i^5}. \tag{59}$$

f is the friction factor that is respectively calculated using Eqs. (60) and (61) for laminar and turbulent flows:

Laminar flow:

$$f = \frac{16}{\text{Re}}. \tag{60}$$

Turbulent flow:

$$f = \frac{0.046}{\sqrt{\text{Re}}}. \tag{61}$$

The total entropy generation may be written in Eq. (62):

$$S_{gen,\text{total}} = S_{gen,\Delta T} + S_{gen,\Delta p} = \frac{Q \Delta T}{T_{f,m}^2 (1+\chi)} + \frac{\dot{m}_f \Delta p}{\rho_f T_{f,m}}. \tag{62}$$

Bejan [32] suggested the non-dimensional form of entropy generation (entropy generation number (EGN)) as follows:

$$EGN = \frac{S_{gen,\text{total}} T_{f,m}}{Q}. \tag{63}$$

The current study studies the effect of variations in borehole length (h), mass flow rate ($\dot{m}$), borehole radius (r_b), and pipe outlet radius (r_{po}) on EGN. The variation ranges of these parameters are determined based on the recommended values of practical engineering projects, as summarized in Table 2 [33]. Figures 12–15 present the EGN variations parallel to the changes of the mentioned parameters to be optimized through the EGN-based optimization process while keeping other parameters constant and this process is affected by the values of the parameters for the design data provided in Table 1 and the variation ranges of each design parameter given in Table 2.

Table 2. Ranges of the design parameters of vertical U-tube heat exchangers [33].

h	40 m to 200 m
$\dot{m}$	0.05 kg/s to 1 kg/s
r_b	0.03 m to 0.5 m
r_{po}	0.014 m to 0.022 m

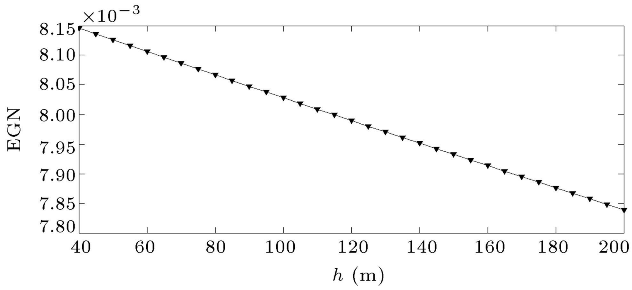

Figure 12. Entropy Generation Number (EGN) vs. borehole lengths.

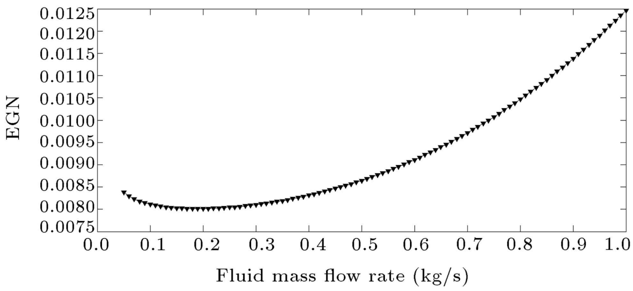

Figure 13. Entropy Generation Number (EGN) vs. fluid mass flow rate.

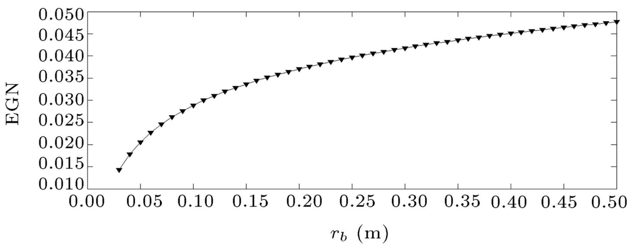

Figure 14. Entropy Generation Number (EGN) vs. borehole radius.

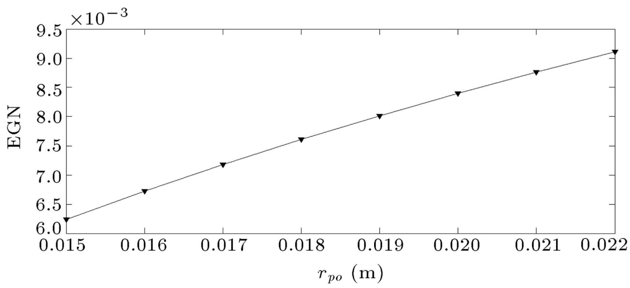

Figure 15. Entropy Generation Number (EGN) vs. pipe outer radius.

It is seen that EGN decreases with an increase in borehole length and also, increases upon increase in the borehole radius and the outer pipe radius.

The optimum parameters are evaluated using the genetic algorithm method. The objective function is EGN that should be minimum. Table 3 shows the comparison between optimum quantities and the primary specifications (Table 1) of the considered borehole.

Table 3. Comparison between optimum parameters and the primary specifications of the considered borehole.

Parameter	Optimum quantity	Primary specification
h	198.6 m	50 m
$\dot{m}$	0.0655 kg/s	0.355 kg/s
r_b	0.05 m	0.1 m
r_{po}	0.015 m	0.016 m
q	16.08 W/m	20.51 W/m
Q	3192.7 W	1025.4 W
Re	4788.7	25947
EGN	0.0052	0.0084

5. Conclusion

In this study, an analytical model based on Green's function was presented. In this model, one-dimensional and two-dimensional heat transfer with a constant borehole wall temperature was assumed. The prediction of borehole heat performance was important as small sizing would lead to a borehole with improper heat performance. Moreover, over sizing led to increase in the cost. To validate the analytical solution, the results of calculated heat transfer rate per unit lengths of 1D and 2D were compared with each other and also, with the experimental data. This comparison showed good agreement between analytical and experimental data. Therefore, borehole heat performance might be predicted based on the analytical solution.

Heat transfer rate per unit length and also temperature distribution around the borehole were evaluated using 1D and 2D models. It was concluded that heat transfer rate per unit length would decrease over time due to the increasing temperature around the borehole. Temperature distribution around the borehole showed that in each location, temperature increased with operating time and for each time step, ground temperature around the borehole decreased to T_0 by taking the distance from the borehole. In the case of more time steps, the distance would become greater due to heat penetration. These results were compatible with findings of Dehghan and Kukrer [9]. Furthermore, after validating analytical solutions, the 6-month nonstop performance of the borehole was predicted.

Flow regime might affect the heat performance of the borehole. In this study, different fluid mass flow rates were examined to have laminar and turbulent flows. It was deduced that q would be approximately constant in laminar flow and for turbulent flow, q was increased following an increase in fluid mass flow rate while it was not linearly proportional.

Borehole length is one of the most important parameters that can affect its performance. In this study, the effect of length on q and Q was evaluated and it was found that q decreased following an increase in borehole length, while Q increased.

Entropy generation number of the borehole was studied and it was concluded that for the considered borehole, entropy generation number was decreased by increasing its length and decreasing the borehole radius and pipe outer radius.

Acknowledgement

The financial support of this research, provided by Iran National Science Foundation (INSF), through Grant No. 88000620 is greatly appreciated.

Nomenclature

c_p	Heat capacity (J/kg K)
EGN	Entropy Generation Number
G	Green's function
h_i	Convective heat transfer coefficient (W/m^{2}K)
h	Borehole depth (m)
$\bar{h}$	Non-dimensional borehole depth
J_0	First kind Bessel's function of zeroth order
J_1	First kind Bessel's function of 1st order
k	Thermal conductivity (W/m K)
l	Far field distance (m)
$\dot{m}$	Fluid mass flow rate (kg/s)
Nu	Nusselt number
q	Heat transfer rate per unit length (W/m)
$\bar{q}$	Non-dimensional heat transfer rate per unit length
Q	Heat transfer rate (W)
r	Radius (m)
$\bar{r}$	Non-dimensional radius
Re	Reynolds number
T	Temperature (C)
$\bar{T}$	Non-dimensional temperature
t	Time
$\bar{t}$	Non-dimensional time
Y_0	Second kind Bessel's function of zeroth order
Y_1	Second kind Bessel's function of 1st order
z	Depth (m)
$\bar{z}$	Non-dimensional depth

Greek letters

α	Thermal diffusivity (m^2/s)
β	Eigenvalue
μ	Fluid dynamic viscosity (kg/ms)
ρ	Density (kg/m^3)

Subscripts

avr.	Averaged value
b	Borehole
eq	Equivalent
f	Fluid
in	Inlet
out	Outlet
pi	Inner pipe
po	Outer pipe
s	Steady state

References

1. Ingersoll, L.R. and Plass, H.J. "Theory of the ground pipe heat source for the heat pump", *Heating, Piping and Air Conditioning*, **20**(7), pp. 119–122 (1948).
2. Carslaw, H.S. and Laeger, J.C., *Conduction of Heat in Solids*, 2nd Edn., Oxford, Oxford University Press, pp. 300–450 (1947).
3. Eskilson, P. "Thermal analysis of heat extraction boreholes", Ph. D Thesis, University of Lund, Sweden, Lund, p. 100 (1948).
4. Zeng, H.Y., Diao, N.R., and Fang, Z.H. "A finite line-source model for boreholes in geothermal heat exchangers", *Heat Transfer-Asian Research*, **31**(7), pp. 558–567 (2002).
5. Aydin, M., Onur, M., and Sisman, A. "A new method for constant temperature thermal response tests", In *42th Workshop on Geothermal Reservoir Engineering*, Standford, California, pp. 13–16 (2017).
6. Biglarian, H., Abbaspour, M., and Saidi, M.H. "A numerical model for transient simulation of borehole heat exchangers", *Renewable Energy*, **104**(7), pp. 224–234 (2017).
7. Lee, C.K. and Lam, H.N. "Computer simulation of borehole ground heat exchangers for geothermal heat pump systems", *Renewable Energy*, **33**(6), pp. 1286–1296 (2008).
8. Minaei, A. and Marefat, M. "A new analytical model for short-term borehole heat exchanger based on thermal resistance capacity model", *Energy and Buildings*, **146**, pp. 233–242 (2017).
9. Dehghan, B. and Kukrer, E. "A new 1D analytical model for investigating the long term heat transfer rate of a borehole ground heat exchanger by Green's function method", *Renewable Energy*, **108**, pp. 615–621 (2017).
10. Man, Y., Yang, H., Diao, N., Liu, J., and Fang, Z. "A new model and analytical solutions for borehole and pile ground heat exchangers", *International Journal of Heat and Mass Transfer*, **53**(13), pp. 2593–2601 (2010).
11. Dehghan, B. "Thermal conductivity determination of ground by new modified two dimensional analytical models: Study cases", *Renewable Energy*, **118**, pp. 393–401 (2018).
12. Lee, C. and Lam, H. "Application of variable-speed ground-source heat pumps to displacement ventilation systems for use in sub-tropical regions", *Building Services Engineering Research & Technology*, **35**(6), pp. 671–681 (2014).
13. Saeidi, V., Mafi, M., and Mohammadi, A. "Development of geothermal heat pumps by using environment friendly refrigerants", *Journal of Renewable and Sustainable Energy*, **10**(1), pp. 1–13 (2018).
14. Kummert, M. and Bernier, M. "Sub-hourly simulation of residential ground coupled heat pump systems", *Building Services Engineering Research & Technology*, **29**, pp. 27–44 (2008).
15. Beier, R.A. and Holloway, W.A. "Changes in the thermal performance of horizontal boreholes with time", *Applied Thermal Engineering*, **78**(1), pp. 1–8 (2015).
16. Mensah, K., Jang, Y.S., and Choi, J.M. "Assessment of design strategies in a ground source heat pump", *Energy and Buildings*, **138**, pp. 301–308 (2017).
17. Cimmino, M. "Fluid and borehole wall temperature profiles in vertical geothermal boreholes with multiple U-tubes", *Renewable Energy*, **96**, pp. 137–147 (2016).
18. Dehkordi, S.E., Schincariol, R.A., and Reitsma, S. "Thermal performance of a tight borehole heat exchanger", *Renewable Energy*, **83**, pp. 698–704 (2015).
19. Tang, F. and Nowamooz, H. "Long-term performance of a shallow borehole heat exchanger installed in a geothermal field of Alsace region", *Renewable Energy*, **128**, pp. 210–222 (2018).
20. Monzó, P., Puttige, A.R., Acuña, J., Mogensen, P., Cazorla, A., Rodriguez, J., Montagud C., and Cerdeira, F. "Numerical modeling of ground thermal response with borehole heat exchangers connected in parallel", *Energy & Buildings*, **172**, pp. 371–384 (2018).
21. Zhang, C., Hu, S., Liu Y., and Wang, Q. "Optimal design of borehole heat exchangers based on hourly load simulation", *Energy*, **116**, pp. 1180–1190 (2016).
22. Li, Y., Han, X., Xiaosong, Z., Geng S., and Li, C. "Study the performance of borehole heat exchanger considering layered subsurface based on field investigations", *Applied Thermal Engineering*, **126**, pp. 296–304 (2017).
23. Holmberg, H., Acuna, J., Næss, E., and Sønju, O.K. "Thermal evaluation of coaxial deep borehole heat exchangers", *Renewable Energy*, **97**, pp. 65–76 (2016).
24. Beier, R.A., Mitchell, M.S., Spitler, J.D., and Javed, S. "Validation of borehole heat exchanger models against

multi-flow rate thermal response tests", *Geothermics*, **71**, pp. 55–68 (2018).

25. Aydin, M. and Sisman, A. "Experimental and computational investigation of multiU-tube boreholes", *Applied Energy*, **145**, pp. 163–171 (2015).

26. Marzbanrad, J., Sharifzadegan, A., and Kahrobaeian, A. "Thermodynamic optimization of GSHPS heat exchangers", *International Journal of Thermodynamics*, **10**(3), pp. 107–112 (2007).

27. Cole, K.D., Haji-Sheikh, A., Beck, J.V., and Litkouhi, B., *Heat Conduction Using Green's Function*, 2nd Edn., CRC press Taylor & Francis Group, p. 544 (2011).

28. Abbasbandy, S. "Modified homotopy perturbation method for nonlinear equations and comparison with Adomian decomposition method", *Applied Mathematics and Computation*, **172**(1), pp. 431–438 (2006).

29. Ozisik, M.N., *Heat Conduction*, 2nd Edn., John Wiley & Sons, p. 226 (1993).

30. Javed, S. and Spitler, J. "Accuracy of borehole thermal resistance calculation methods for grouted single U-tube ground heat exchangers", *Applied Energy*, **187**, pp. 790–806 (2017).

31. Holman, J.P., *Heat Transfer*, 10th Edn., McGraw-Hill Book Company, p. 280 (2010).

32. Bejan, A., *Entropy Generation Minimization: The Method of Thermodynamic Optimization of Finite-Size Systems and Finite-Time Processes*, 1st Edn., CRC Press, pp. 113–138 (1996).

33. ASHRAE, HVAC application SI handbook, *HVAC Applications Handbook*, SI Edn., ASHRAE, pp. 34.1–34.34 (2011).

Biographies

Masoud Mohammadian Korouyeh is a PhD Candidate at Islamic Azad University, Tehran Science and Research Branch, Tehran, Iran. His research interests include heat transfer in refrigeration systems, modeling of boreholes, desiccant cooling systems, and renewable energy application.

Mohammad Hassan Saidi is a Professor of Mechanical Engineering at Sharif University of Technology, Tehran, Iran. His current research interests include heat transfer enhancement in boiling and condensation, combustion modeling and simulation, modeling of pulse refrigeration, vortex tube refrigerators, modeling of boreholes, indoor air quality and clean room technology, and energy efficiency of home appliances and desiccant cooling systems.

Mohammad Najafi is an Associated Professor of Mechanical Engineering at Islamic Azad University, Tehran Science and Research Branch, Tehran, Iran. He received his PhD degree in Mechanical Engineering, Thermal Fluids in 1989 from the University of Alabama, USA. His current research interests include energy modeling, heat transfer enhancement in refrigeration systems, desiccant cooling systems, and non-Newtonian fluid.

Cyrus Aghanajafi is a Professor of Mechanical Engineering at Khaje Nasir Toosi University of Technology, Tehran, Iran. His current research interests include heat transfer modeling in energy systems, thermodynamic analysis, fluid flow, and radiation heat transfer.